



Humanized NOD/SCID/IL2 γ ^{null} (hu-NSG) Mouse Model for HIV Replication and Latency Studies

Xin Xia¹, Haitang Li¹, Sangeetha Satheesan^{1,2}, Jiehua Zhou¹, and John J. Rossi¹

¹Department of Molecular and Cellular Biology, Beckman Research Institute of City of Hope

²Irell and Manela Graduate School of Biological Sciences, Beckman Research Institute of City of Hope

Abstract

Ethical regulations and technical challenges for research in human pathology, immunology, and therapeutic development have placed small animal models in high demand. With a close genetic and behavioral resemblance to humans, small animals such as the mouse are good candidates for human disease models, through which human-like symptoms and responses can be recapitulated. Further, the mouse genetic background can be altered to accommodate diverse demands. The NOD/SCID/IL2 γ ^{null} (NSG) mouse is one of the most widely used immunocompromised mouse strains; it allows engraftment with human hematopoietic stem cells and/or human tissues and the subsequent development of a functional human immune system. This is a critical milestone in understanding the prognosis and pathophysiology of human-specific diseases such as HIV/AIDS and aiding the search for a cure. Herein, we report a detailed protocol for generating a humanized NSG mouse model (hu-NSG) by hematopoietic stem cell transplantation into a radiation-conditioned neonatal NSG mouse. The hu-NSG mouse model shows multi-lineage development of transplanted human stem cells and susceptibility to HIV-1 viral infection. It also recapitulates key biological characteristics in response to combinatorial antiretroviral therapy (cART).

Keywords

Immunology and Infection; Issue 143; Neonatal NSG mouse; Humanized mice; HSCs; HIV; cART; Latency

Introduction

Because establishing suitable animal models for human diseases is key to finding a cure, appropriate animal models have long been pursued and improved over time. Multiple strains of immunocompromised murine models have been developed that permit the engraftment of human cells and/or tissues and the subsequent execution of humanized

Correspondence to: Xin Xia at xixia@coh.org.

Disclosures

The authors disclose no conflicts of interest.

Video link

The video component of this article can be found at <https://www.jove.com/video/58255/>

functions^{1,2}. Such humanized mouse models are critical for investigations of human-specific diseases^{3,4,5}.

Acquired immune deficiency syndrome (AIDS) resulting from infection with human immunodeficiency virus (HIV) is one example. Prior to the establishment of humanized mouse models, ethical and technical limitations confined HIV/AIDS preclinical animal studies to non-human primates³. However, the high expenses and requirements for specialized care for such animal hinder HIV/AIDS studies in typical academic settings. HIV primarily infects human CD4+ T-cells and impacts the development and immune responses of other human immune cells such as B-cells, macrophages, and dendritic cells⁶; therefore, small animal models transplanted with functional human immune systems are in high demand.

A breakthrough came in 1988, when CB17-scid mice with a *Prkdc^{scid}* mutation were developed and showed successful engraftment of the human immune system¹. The *Prkdc^{scid}* mutation results in defective T- and B-cell functions and an ablated adaptive immune system in mice, thereby enabling the engraftment of human peripheral blood mononuclear cells (PBMCs), hematopoietic stem cells (HSCs), and fetal hematopoietic tissues^{7,8}. Nonetheless, low levels of engraftment are frequently observed in this model; possible causes are 1) residual innate immune activity modulated via natural killer (NK)-cells and 2) the late-stage development of mouse T- and B-cells (leakiness)⁵. The subsequent development of the non-obese diabetic (NOD)-scid mouse model achieved dramatic down-regulation of NK-cell activity; thus, it is able to support a higher level and more sustainable engraftment of human immune system components⁹. To further suppress or impede development of innate immunity, mouse models bearing truncation or total knockout of the interleukin-2 receptor γ -chain (*Il2rg*) in the (NOD)-*scid* background were established. *Il2rg*, also known as common cytokine-receptor γ -chain, is an indispensable component of various cytokine receptors^{10,11,12,13}. Strains such as NOD.Cg-*Prkdc^{scid}Il2rg^{tm1Wji}* (NSG) and NODShi.Cg-*Prkdc^{scid}Il2rg^{tm1Sug}* (NOG) present robust disruption of mouse cytokine signaling and complete ablation of NK-cell development, in addition to severe impairment of adaptive immunity^{14,15,16}.

Three humanized mouse models bearing a *scid* mutation and *Il2rg* knockout are frequently employed in HIV/AIDS research: the BLT (Bone marrow/Liver/Thymus) model, the PBL (Peripheral Blood Leukocyte) model, and the SRC (SCID Repopulating Cell) model³. The BLT model is created via surgical transplantation of human fetal liver and thymus under the mouse kidney capsule accompanied with intravenous injection of fetal liver HSCs^{3,17,18}. The BLT mouse model offers high engraftment efficacy, development of human hematopoietic cells in all lineages, and establishment of a strong human immune system; additionally, T-cells are educated in a human autologous thymus and exhibit HLA-restricted immune responses^{4,5,17,19}. However, the requirement for surgical procedures remains the major drawback of the BLT model. The PBL mouse model is established by intravenous injection with human peripheral lymphoid cells. The PBL model offers convenience and yields successful T-cell engraftment, but its application is limited due to insufficient B-cell and myeloid cell engraftment, low engraftment levels overall, and the onset of severe graft-versus-host disease (GVHD)^{3,20}. The SRC mouse model is established through injection of

human HSCs into newborn or young adult SCID mice. It exhibits average engraftment efficiency above 25% (assessed as peripheral blood CD45 percentage) and supports the multiple-lineage development of injected HSCs and the elaboration of an innate human immune system. However, the limitation of the SRC model is that the T-cell response is mouse H2-restricted instead of human HLA-restricted^{14,21}.

The SRC mouse model is considered a facile and reliable model for preclinical HIV/AIDS small animal studies, exemplified by the consistent engraftment of a human immune system and successful hematopoietic development. We previously reported the establishment of a NSG Hu-SRC-SCID (hu-NSG) mouse model and described its application in HIV replication and latency studies^{22,23,24}. This hu-NSG mouse model exhibits high levels of bone marrow homing, susceptibility to HIV infection, and recapitulation of HIV infection and pathogenesis. Additionally, the hu-NSG mouse model responds appropriately to combinatorial antiretroviral therapy (cART) and recapitulates plasma viral rebound upon cART withdrawal, confirming the establishment of an HIV latency reservoir^{25,26,27}. This HIV latency reservoir is further substantiated by the production of replication-competent HIV viruses *ex vivo* induced by human resting CD4+ T-cells isolated from infected and cART-treated hu-NSG mice.

Herein, we describe the detailed protocol for establishment of the hu-NSG mouse model from neonatal NSG mice, including procedures related to HIV infection and cART treatment for latency development. We expect this protocol to offer a new set of approaches in HIV animal studies regarding HIV virology, latency, and treatment.

Protocol

All animal care and procedures have been performed according to protocols reviewed and approved by the City of Hope Institutional Animal Care and Use Committee (IACUC) held by the principal investigator of this study (Dr. John Rossi, IACUC #12034). Human fetal liver tissue was obtained from Advanced Bioscience Resources (Alameda, CA), a nonprofit organization, in accordance with federal and state regulations. The vendor has its own Institutional Review Board (IRB) and is compliant with human subject protection requirements. Human PBMCs are isolated from discarded peripheral blood specimens from anonymous healthy donors from City of Hope Blood Donor Center (Duarte, CA), with no identification regarding age, race, gender, or ethnicity. IRB#/REF#: 97071/075546

1. General Aseptic Practice

1. Perform tissue culture experiments in designated laminar flow cabinets.
2. Keep tissue culture medium and supplements under sterile conditions and filter using a 0.22- μ m filtration unit prior to use.
3. Preserve prepared human HSCs in sterile tubes and keep on ice until injection.
4. As a result of severe immune deficiency, handle NSG mice aseptically. Wear a disposable surgery gown, hair cap, face mask, shoe covers, and gloves to prevent contamination. Sanitize the bench surface, irradiation holder, and induction

chamber for anesthesia with chlorine dioxide based sterilant (*e.g.*, Clidox) before and after experiments.

5. Apply petroleum-based eye ointment after retro-orbital bleeding to prevent dry eyes.
6. Change to antibiotic-containing diet to prevent infection due to retro-orbital bleeding.

2. Handling HIV Virus, Infected Rodents, and Virus-containing Blood/Tissue Samples

CAUTION: HIV is a class 3 human pathogen; the handling rules must be followed exactly.

1. Handle HIV virus-containing samples in a designated BSL2+/3 laboratory space. Lock virus-containing reagents securely in a secondary container during transportation. Disinfect the outer surface of all containers by thorough wiping with 10% bleach and isopropanol prior to transportation.
2. Keep all virus-containing wastes in designated waste containers with 2–3 layers of biohazardous waste bags. Prior to waste disposal, disinfect by generously spraying the waste with iodine/ethoxylated nonylphenol solution (*e.g.*, Wescodyne) and autoclave.
3. Wear personal protective equipment: hair cap, face cover, anti-splash face shield, shoe covers, disposable surgery gown, and double-layer gloves.
4. Handle infected rodents with extreme caution. Conduct injections and blood collections while mice are under anesthesia (Steps 5.1–5.2, 6.3–6.5, 7.3, and 8.1–8.2).

3. Isolation of Hematopoietic Stem Cells

1. Prepare collagenase/dispase solution for tissue digestion.
 1. Dissolve collagenase/dispase powder to make stock solution at a concentration of 100 mg/mL, and store collagenase/dispase stock solution in 150 μ L aliquots at -20°C .
 2. For working collagenase solution, dilute 150 mL of collagenase/dispase stock with 15 mL of RPMI 1640 supplemented with 10% FCS and 1% penicillin/streptomycin.

NOTE: The final concentration of collagenase/dispase for tissue digestion is 1 mg/mL.

2. With a sterile razor blade, cut fetal liver tissue (16–24 weeks gestation) into small pieces (approximately 2–3 mm³ in size) followed by digestion with collagenase/dispase solution (1 mg/mL) for 30 minutes at room temperature. Adjust the volume of digestion solution so that all tissue pieces are fully

submerged. Use the back end of the syringe plunger to gently grind the tissue sample to facilitate digestion.

3. Pass the digestion mixture through a 70- μm sterile nylon mesh filter to acquire a single cell suspension.
4. Enrich for CD34+ HSCs using a MACS system per manufacturer's instruction.
5. Count the viable percentage of enriched CD34+ HSCs using a hemacytometer²⁸ and proceed to intrahepatic injection into neonatal NSG mice.
6. Freeze the remaining enriched CD34+ HSCs in freezing media (*e.g.*, CryoStor CS2) and preserve cells in a liquid nitrogen tank. Upon future use, recount the viable percentage of thawed CD34+ HSCs prior to injection. With the use of freezing media, post-thaw viability is between 80 to 90%.

4. Intrahepatic Injection of Human CD34+ HSCs in Neonatal NSG Mice

NOTE: Neonatal NSG mice 2–3 days from birth are most suitable for this procedure, as they are strong enough to endure irradiation at half-lethal dose, while young enough to have totally impaired immune systems. No anesthesia is required for the HSC injection.

1. Place the whole litter of neonatal NSG mice (typically 5–10 mice, both genders) in a sterile pie-shaped irradiation cage and expose to a total dose of 200–250 cGy gamma-ray radiation from a Caesium-137 radiation source. Ensure that radiation dose is within the range, as significant weight loss or even death can be observed when NSG mice are exposed to high doses of irradiation.¹²

NOTE: Radiation is a health hazard, personal protection against radiation should be taken.

2. Following irradiation, inject each neonatal NSG mouse with 5×10^5 viable human CD34+ HSCs using a syringe/needle setup (Figure 1). Directly inject cells into the liver.

5. Engraftment Validation Through Retro-Orbital Bleeding and Flow Cytometry Analysis

1. At 10–12 weeks post-HSC injection, anesthetize mice using an isoflurane/oxygen inhalation apparatus. Adjust the oxygen flow to maintain isoflurane percentage at 4–5%. Anesthesia takes 3–5 minutes, depending on individual mouse. Properly anesthetized mice show a slow and deep breathing pattern, and no reaction to toe-pinching stimulation.
2. Collect 50–100 μL of peripheral blood from each mouse through retro-orbital sampling²⁸. Store blood samples in K2EDTA or heparinized blood collection tubes to prevent coagulation.

NOTE: Blood collection tubes are required to have anticoagulant coating so that mouse PBMCs can be isolated from whole blood for flow cytometry analysis.

EDTA is known to inhibit enzymatic reactions such as PCR and qRT-PCR; thus, if downstream enzymatic reactions are required, use a heparinized blood collection apparatus.

3. Centrifuge blood samples at $2,000 \times g$ for 20 minutes at 4°C to pellet blood cells.
 1. Transfer the plasma supernatants to new microcentrifuge tubes after centrifugation and store at -80°C if cytokine analysis is required.
 2. Lyse the red blood cells (RBCs) within the blood cell pellet at room temperature for 10 minutes using Red Blood Cell Lysis Buffer (Table of Materials).

NOTE: If plasma samples are not required, directly lyse the whole blood with lysis solution without centrifugation.

4. Pellet remaining blood cells after RBC lysis at $300 \times g$ for 5 minutes at 4°C ; aspirate the supernatant. Wash the cell pellets with 0.01 % BSA containing DPBS, centrifuge at $300 \times g$ for 5 minutes at 4°C and aspirate supernatant. Repeat the washing step one more time.
5. Block cells with 100 μL of $1\times$ blocking cocktail (Table 3 for recipe) for 20 minutes at 4°C .
6. After blocking, directly add each antibody solution into the cell suspension at a concentration of $2 \mu\text{L}/10^6$ cells and incubate at 4°C for 30 minutes. Antibodies for engraftment validation are: anti-human CD45 (leukocytes, RRID: AB_2732068), anti-human CD3 (T-cells, RRID: AB_396896), anti-human CD4 (helper T-cells, RRID: AB_397037), anti-human CD8 (cytotoxic T-cells, RRID: AB_2722501), anti-human CD14 (monocytes, RRID: AB_10373536), and anti-human CD19 (B-cells, RRID: AB_10373382). For suggested flow panel, please see Table 4 and Table of Materials for catalog numbers, RRIDs and lot numbers.

NOTE: Antibody staining in blocking solution eliminates non-specific binding of the anti-human antibodies toward mouse surface markers, as several surface markers share homology between human and mouse.

7. Isolate human PBMCs from healthy donors and prepare single-stained flow cytometry compensation controls using purified human PBMCs. Alternatively, use fluorescence-labeled microspheres as compensation controls²⁹.
8. Analyze the peripheral blood samples using a flow cytometer and quantify the percentage of human CD45+ cells, human CD3+ cells, human CD14+ cells, and human CD19+ cells from total peripheral blood cells.
 1. For downstream HIV infection and latency studies, calculate the percentage of CD4+ T-cells and CD8+ T-cells within the CD3+ cells.

NOTE: Typically, a CD4:CD8 ratio between 1.5 and 2.5 is observed prior to HIV infection³⁰.

6. Analysis of HIV Infection of hu-NSG Mice and Plasma Viral Load Using qRT-PCR

1. Propagate HIV BaL viral stock in human PBMCs from healthy donors, harvest at day 10 post-infection, and titrate using p24 ELISA kit³¹.
2. Select hu-NSG mice with more than 20% human CD45+ cells in the peripheral blood for HIV infection.
3. Anesthetize hu-NSG mice using an isoflurane/oxygen inhalation apparatus (Step 5.1).
4. After confirming animal is anesthetized, inject HIV BaL virus at a dose of 200 ng of p24 per mouse through intraperitoneal route.

NOTE: Be extremely cautious with the needle, do not reuse needles, and discard immediately after use into designated sharp container. Disinfect the area of injection after virus administration.

5. Three weeks post-infection, anesthetize hu-NSG mice and collect peripheral blood through retro-orbital bleeding using heparinized capillary tubes and collection tubes.
6. Separate plasma and blood cells by centrifugation at $2,000 \times g$ for 20 minutes.
7. Lyse RBCs. Block and stain remaining blood cells with antibodies for flow cytometry analysis (Section 5.3–5.8).

NOTE: Flow cytometry analysis should focus on comparing CD4:CD8 ratio before and after infection. Significant decrease in CD4+ cell count is expected, as the CD4 antigen serves as a co-receptor for viral entry.

8. Use plasma samples to analyze the HIV viral load using qRT-PCR. Isolate viral RNA from plasma samples using a viral RNA mini kit. Perform qRT-PCR with HIV-1 LTR-specific primers and probe sets (sequence details in Table 5), using manufacturer's protocol.

7. Oral Administration of cART and Validation of Viral Suppression (optional)

NOTE: This step is optional for investigations regarding HIV prognosis, virology, or infection-related pathophysiology during the acute infection phase. cART treatment of HIV-infected hu-NSG is used to recapitulate HIV latency among human patients receiving cART. Successfully HIV-infected hu-NSG mice are given cART for 4 weeks. The cART regimen consists of tenofovir disoproxil fumarate (TDF; 300 mg/capsule), emtricitabine (FTC; 200 mg/capsule), and raltegravir (RAL; 400 mg/capsule). The dose of cART for treating HIV-infected hu-NSG mice is adjusted according to body surface area (Table 1, Equation 1, Table 2)³².

1. Calculate the amount of each medication required for each cage during one week of treatment, taking into consideration the volume of the water bottle, the number of mice in each cage, and an average daily water intake of 4 mL per mouse.

NOTE: The key point in this step is to ensure that each mouse acquires its daily dose within 4 mL of drinking water.

2. Grind all three medications with adjusted doses into fine powder and dissolve the powder mixture in sweetened water (*e.g.*, Medidrop Suralose). Change the water bottle every week with freshly dissolved cART cocktail supplied in sweetened water.

NOTE: The drug powder may not dissolve immediately, shake vigorously to achieve a homogeneous suspension before returning the bottle to the holding cage.

3. Collect peripheral blood samples via retro-orbital bleeding every two weeks and analyze both the CD4:CD8 ratio using flow cytometry (Section 5.3–5.8) and the plasma viral load using qRT-PCR (Section 6.6).

NOTE: Typically after 4 weeks of treatment, the plasma viral load decreases to below the detection limit and a typical CD4:CD8 ratio is restored.

8. Validation of Viral Rebound upon cART Withdrawal (optional)

NOTE: This step is critical in validating the latency model, as viral rebound upon cART withdrawal provides direct evidence of a latency reservoir. It is also recommended to serve as a control experiment for therapeutic investigations on HIV rebound suppressants.

1. Plan for cART withdrawal after plasma viral loads from peripheral blood samples are below the detection limit and the CD4:CD8 ratio is restored to a range between 1.5 and 2.5.
2. Collect peripheral blood samples through retro-orbital bleeding every 2 weeks after cART withdrawal. Closely monitor the change in plasma viral loads (Section 6.6) as well as the CD4:CD8 ratio (Section 5.3–5.8).

Representative Result

Flow cytometry analysis is frequently performed to validate the purity of isolated HSCs, evaluate engraftment levels, profile immune responses to viral infection, and survey cART efficacy. A typical antibody panel contains 4–6 individual fluorescently labeled antibodies; thus, a flow cytometer with multiple lasers and a wide selection of filters is crucial for achieving accurate results.

For initial engraftment validation, the human CD45⁺ cell count can range from 20% to 80%, and subsets of human leukocytes should appear as discrete populations on the flow dot-plot (Figure 2). The ratio of CD4:CD8 stays between 1.5 and 2.5 for a healthy individual; significant CD4⁺ depletion is typically observed upon viral infection, yielding a lower ratio

of CD4:CD8; and restoration of the healthy ratio is observed upon cART treatment (Figure 3).

qRT-PCR gives a detection limit of 40 RNA copies/mL of plasma; proper dilutions are required prior to the experiment. Plasma viral loads detected using qRT-PCR throughout the course of the infection and cART regimen can be plotted and used to evaluate the efficiency of infection and cART (Figure 4).

$$\begin{aligned} & \text{Human Dose (mg/kg)} \\ &= \text{Animal equivalent dose (mg/kg)} \times \frac{\text{Animal } K_m \text{ factor}}{\text{Human } K_m \text{ factor}} \end{aligned}$$

Equation 1. Dose translation based on body surface area (BSA).

Equation for translating human dose to dosing against small experimental animals. The K_m factor can be found in Table 2.

Discussion

Immunocompromised mice engrafted with human cells/tissue present human-like physiological characteristics and are a tremendous value for pathology, pathophysiology, and immunology studies concerning human-specific diseases. Among multiple strains of immunocompromised mice, the NOD.Cg-*Prkdc*^{scid}*Il2r*^{tm1Wji}(NSG) model is the most immunodeficient due to its lack of both innate and adaptive immunity, as well as ablated mouse-specific cytokine signaling^{3,12,19}. Therefore, NSG mice have been extensively utilized in the humanization process, and it is well established that human cells repopulate in the murine peripheral blood, lymphoid and myeloid tissues, and that the mice exhibit appropriate human immune responses to infectious stimulations such as HIV^{27,33}.

Due to the host restriction of HIV, preclinical animal studies of HIV virology and infection prognosis were previously limited to non-human primates infected with simian immunodeficiency virus (SIV, the non-human primate version of HIV)³. Scientific advancements in stem cell research and the generation of NSG mice have opened up the possibility of conducting HIV research on small murine animals with lower cost and faster experimental turnover. Currently, NSG humanization can be achieved through transplantation of 1) fetal tissues and human HSCs (BLT model), 2) human PBMCs (PBL model), and 3) human HSCs (SRC model). The BLT model offers the highest engraftment efficiency as well as comprehensive development of both lymphoid and myeloid functions^{34,35}, but is technically demanding. The PBL model is the most convenient to establish but has a short experimental window upon engraftment resulting from GVHD; additionally it only offers decent peripheral T-cell responses and lacks lymphoid and myeloid development. For these reasons, we employed the SRC model in this protocol, with adaptations to meet the requirements for HIV investigations. The hu-NSG model is completely devoid of immune function and efficient at bone marrow homing upon radiation and transplantation; furthermore, it allows viral challenge and subsequent investigations at a younger age, avoiding the development of age-related pathological problems known to the NOD strain

background. Although T-cells in the hu-NSG model are educated in a mouse thymic environment and are only H2-restricted, multiple, if not all, subsets of human immune cells can develop in and colonize mouse lymphoid and myeloid organs. Noticeably, gut-associated lymphoid tissue of the hu-NSG model is also reconstituted with human immune cells; thus, this model could potentially support HIV mucosal transmission, similar to the BLT model^{22,23}.

One of the major obstacles to eradicating HIV is the existence of a latency reservoir among patients treated with suppressive cART^{33,36,37,38,39}. Latently infected cells remain quiescent, and contribute to HIV viral rebound upon cART withdrawal. Latency reservoirs are anatomically located in the liver, spleen, brain, and other lymphoid tissues, and are mainly composed of memory CD4+ T-cells^{36,40,41}. As reported by our group, the hu-NSG model fully supports development of the T-cell lineage, making it suitable for pathological modeling of HIV latency. We showed this model is highly susceptible to viral infection and subsequently to the cART regimen via oral administration. Dramatic viral rebound occurs immediately upon cART withdrawal, which fully supports the existence of a latency reservoir. Latently infected memory CD4+ T-cells can be isolated from the lymphoid organs of HIV-infected hu-NSG during cART, and viral outgrowth assays recapitulate viral rebound *ex vivo*⁴¹. The hu-NSG model and the HIV infection/cART regimen described in this protocol thus have broad applications in fields related to HIV virology, infection prognosis, latency pathophysiology, and antiretroviral therapeutics development.

The hu-NSG mouse model in this protocol requires irradiation and intrahepatic injection of HSCs at day 2–3 after birth; therefore, in-house breeding and specific housing conditions are required. Although neonatal HSC transplantation generally yields high engraftment efficiencies, in some cases severe GVHD can occur. In some cases, a significant decrease in peripheral CD45+ cell count can be observed upon infection, and in extreme conditions, peripheral blood CD45+ depletion can be observed; therefore, blood collection and flow cytometry analysis can be challenging. One of the major limitations of this hu-NSG mouse model lies within the chimeric nature of its T-cells. T-cells in the hu-NSG mouse model are educated within the mouse thymic environment and are H2-restricted instead of being HLA-restricted; therefore, full recapitulation of the dynamic changes of T-cell subsets upon infection is less likely. Further, although the hu-NSG mouse model exhibits good susceptibility to HIV-1 infection, the observed plasma viral load can be several-fold lower than in the BLT model, possibly due to incomprehensive reconstitution of human lymphoid and myeloid functions.

In summary, the hu-NSG mouse depicted in this protocol offers an easy and efficient methodology for generating a humanized mouse model for HIV virology and latency studies, as an alternative to the BLT model. Despite its limitations in comprehensive lymphoid and myeloid development, the hu-NSG model has been proven susceptible to infection and responsive to cART treatment or other therapeutics^{22,23,24}. The latency pathology model established according to this protocol recapitulates HIV viral rebound *in vivo* and latently infected memory CD4+ T-cells can be further isolated for additional investigation.

Acknowledgements

This work was supported by the National Institutes of Health [grant numbers R01AI29329, R01AI42552 and R01HL07470 to J.J.R.] and National Cancer Institute of the National Institutes of Health [grant number P30CA033572 to support City of Hope Integrative Genomics, Analytical Pharmacology, and Analytical Cytometry Cores]. The following reagent was obtained through the NIH AIDS Research and Reference Reagent Program, Division of AIDS, NIAID, NIH: HIV BaL virus.

Reference

- Greiner DL, Hesselton RA, Shultz LD SCID mouse models of human stem cell engraftment. *Stem cells*. 16 (3), 166–177 (1998). [PubMed: 9617892]
- Rongvaux A et al. Development and function of human innate immune cells in a humanized mouse model. *Nature biotechnology*. 32 (4), 364–372 (2014).
- Walsh NC et al. Humanized Mouse Models of Clinical Disease. *Annual review of pathology*. 12, 187–215 (2017).
- Shultz LD, Brehm MA, Garcia-Martinez JV, Greiner DL Humanized mice for immune system investigation: progress, promise and challenges. *Nature reviews. Immunology*. 12 (11), 786–798 (2012).
- Shultz LD, Ishikawa F, Greiner DL Humanized mice in translational biomedical research. *Nature reviews. Immunology*. 7, 118 (2007).
- Moir S, Fauci AS B cells in HIV infection and disease. *Nature reviews. Immunology*. 9 (4), 235–245 (2009).
- McCune JM, et al. The SCID-hu mouse: murine model for the analysis of human hematolymphoid differentiation and function. *Science*. 241 (4873), 1632–1639 (1988). [PubMed: 2971269]
- Mosier DE, Gulizia RJ, Baird SM, Wilson DB Transfer of a functional human immune system to mice with severe combined immunodeficiency. *Nature*. 335, 256 (1988). [PubMed: 2970594]
- Shultz LD et al. Multiple defects in innate and adaptive immunologic function in NOD/LtSz-scid mice. *Journal of immunology*. 154 (1), 180–191 (1995).
- Ohbo K et al. Modulation of hematopoiesis in mice with a truncated mutant of the interleukin-2 receptor gamma chain. *Blood*. 87 (3), 956–967 (1996). [PubMed: 8562967]
- Ito M et al. NOD/SCID/gamma(c)(null) mouse: an excellent recipient mouse model for engraftment of human cells. *Blood*. 100 (9), 3175–3182 (2002). [PubMed: 12384415]
- Shultz LD et al. Human lymphoid and myeloid cell development in NOD/LtSz-scid IL2R gamma null mice engrafted with mobilized human hemopoietic stem cells. *Journal of immunology*. 174 (10), 6477–6489 (2005).
- Ishikawa F et al. Development of functional human blood and immune systems in NOD/SCID/IL2 receptor {gamma} chain(null) mice. *Blood*. 106 (5), 1565–1573 (2005). [PubMed: 15920010]
- Watanabe Y et al. The analysis of the functions of human B and T cells in humanized NOD/shi-scid/gammac(null) (NOG) mice (hu-HSC NOG mice). *International immunology*. 21 (7), 843–858 (2009). [PubMed: 19515798]
- McDermott SP, Eppert K, Lechman ER, Doedens M, Dick JE Comparison of human cord blood engraftment between immunocompromised mouse strains. *Blood*. 116 (2), 193–200 (2010). [PubMed: 20404133]
- Mazurier F, Doedens M, Gan OI, Dick JE Rapid myeloerythroid repopulation after intrafemoral transplantation of NOD-SCID mice reveals a new class of human stem cells. *Nature medicine*. 9 (7), 959–963 (2003).
- Melkus MW et al. Humanized mice mount specific adaptive and innate immune responses to EBV and TSST-1. *Nature medicine*. 12, 1316 (2006).
- Lan P, Tomomura N, Shimizu A, Wang S, Yang Y-G Reconstitution of a functional human immune system in immunodeficient mice through combined human fetal thymus/liver and CD34+ cell transplantation. *Blood*. 108 (2), 487–492 (2006). [PubMed: 16410443]
- Brehm MA, Bortell R, Verma M, Shultz LD, Greiner DL Humanized Mice in Translational Immunology. *Translational Immunology*. 285–326 (2016).

20. King MA et al. Hu-PBL-NOD-scid Il2rnull mouse model of xenogeneic graft-versus-host-like disease and the role of host MHC. *Clinical & Experimental Immunology*. 157, 104–118 (2009). [PubMed: 19659776]
21. Halkias J et al. Conserved and divergent aspects of human T-cell development and migration in humanized mice. *Immunology and cell biology*. 93 (8), 716–726 (2015). [PubMed: 25744551]
22. Satheesan S et al. HIV replication and latency in a humanized NSG mouse model during suppressive oral combinational ART. *Journal of virology*. (2018).
23. Zhou J et al. Receptor-targeted aptamer-siRNA conjugate-directed transcriptional regulation of HIV-1. *Theranostics*. 8 (6), 1575–1590 (2018). [PubMed: 29556342]
24. Zhou J et al. Cell-specific RNA aptamer against human CCR5 specifically targets HIV-1 susceptible cells and inhibits HIV-1 infectivity. *Chemistry & biology*. 22 (3), 379–390 (2015). [PubMed: 25754473]
25. Brechtel JR, Breitbart W, Galieta M, Krivo S, Rosenfeld B The use of highly active antiretroviral therapy (HAART) in patients with advanced HIV infection: impact on medical, palliative care, and quality of life outcomes. *Journal of pain and symptom management*. 21 (1), 41–51 (2001). [PubMed: 11223313]
26. Richman DD, Margolis DM, Delaney M, Greene WC, Hazuda D, Pomerantz RJ The Challenge of Finding a Cure for HIV Infection. *Science*. 323 (5919), 1304–1307 (2009). [PubMed: 19265012]
27. Pace MJ, Agosto L, Graf EH, O’Doherty U HIV reservoirs and latency models. *Virology*. 411 (2), 344–354 (2011). [PubMed: 21284992]
28. Van Herck H et al. Blood sampling from the retro-orbital plexus, the saphenous vein and the tail vein in rats: comparative effects on selected behavioural and blood variables. *Laboratory animals*. 35 (2), 131–139 (2001). [PubMed: 11315161]
29. Autissier P, Soulas C, Burdo TH, Williams KC Evaluation of a 12-color flow cytometry panel to study lymphocyte, monocyte, and dendritic cell subsets in humans. *Cytometry*. 9999A, NA-NA (2010).
30. Lu W, Mehraj V, Vyboh K, Cao W, Li T, Routy J-P CD4:CD8 ratio as a frontier marker for clinical outcome, immune dysfunction and viral reservoir size in virologically suppressed HIV-positive patients. *Journal of the International AIDS Society*. 18, 20052 (2015). [PubMed: 26130226]
31. van’t Wout AB, Schuitemaker H, Kootstra NA Isolation and propagation of HIV-1 on peripheral blood mononuclear cells. *Nature protocols*. 3, 363 (2008). [PubMed: 18323807]
32. Reagan-Shaw S, Nihal M, Ahmad N Dose translation from animal to human studies revisited. *FASEB journal: official publication of the Federation of American Societies for Experimental Biology*. 22 (3), 659–661 (2008). [PubMed: 17942826]
33. Han Y, Wind-Rotolo M, Yang H-C, Siliciano JD, Siliciano RF Experimental approaches to the study of HIV-1 latency. *Nature reviews. Microbiology*. 5 (2), 95–106 (2007). [PubMed: 17224919]
34. Marsden MD et al. HIV Latency in the Humanized BLT Mouse. *Journal of virology*. 86 (1), 339–347 (2012). [PubMed: 22072769]
35. Karpel ME, Boutwell CL, Allen TM BLT humanized mice as a small animal model of HIV infection. *Current opinion in virology*. 13, 75–80 (2015). [PubMed: 26083316]
36. Durand CM, Blankson JN, Siliciano RF Developing strategies for HIV-1 eradication. *Trends in immunology*. 33 (11), 554–562 (2012). [PubMed: 22867874]
37. Van Lint C, Bouchat S, Marcello A HIV-1 transcription and latency: an update. *Retrovirology*. 10, 67 (2013). [PubMed: 23803414]
38. Xu L, Zhang Y, Luo G, Li Y The roles of stem cell memory T cells in hematological malignancies. *Journal of hematology & oncology*. 8, 113 (2015). [PubMed: 26462561]
39. Chun T-W, Moir S, Fauci AS HIV reservoirs as obstacles and opportunities for an HIV cure. *Nature immunology*. 16 (6), 584–589 (2015). [PubMed: 25990814]
40. Redel L et al. HIV-1 regulation of latency in the monocyte-macrophage lineage and in CD4+ T lymphocytes. *Journal of leukocyte biology*. 87 (4), 575–588 (2010). [PubMed: 19801499]
41. Laird GM et al. Rapid Quantification of the Latent Reservoir for HIV-1 Using a Viral Outgrowth Assay. *PLoS pathogens*. 9 (5), e1003398 (2013).

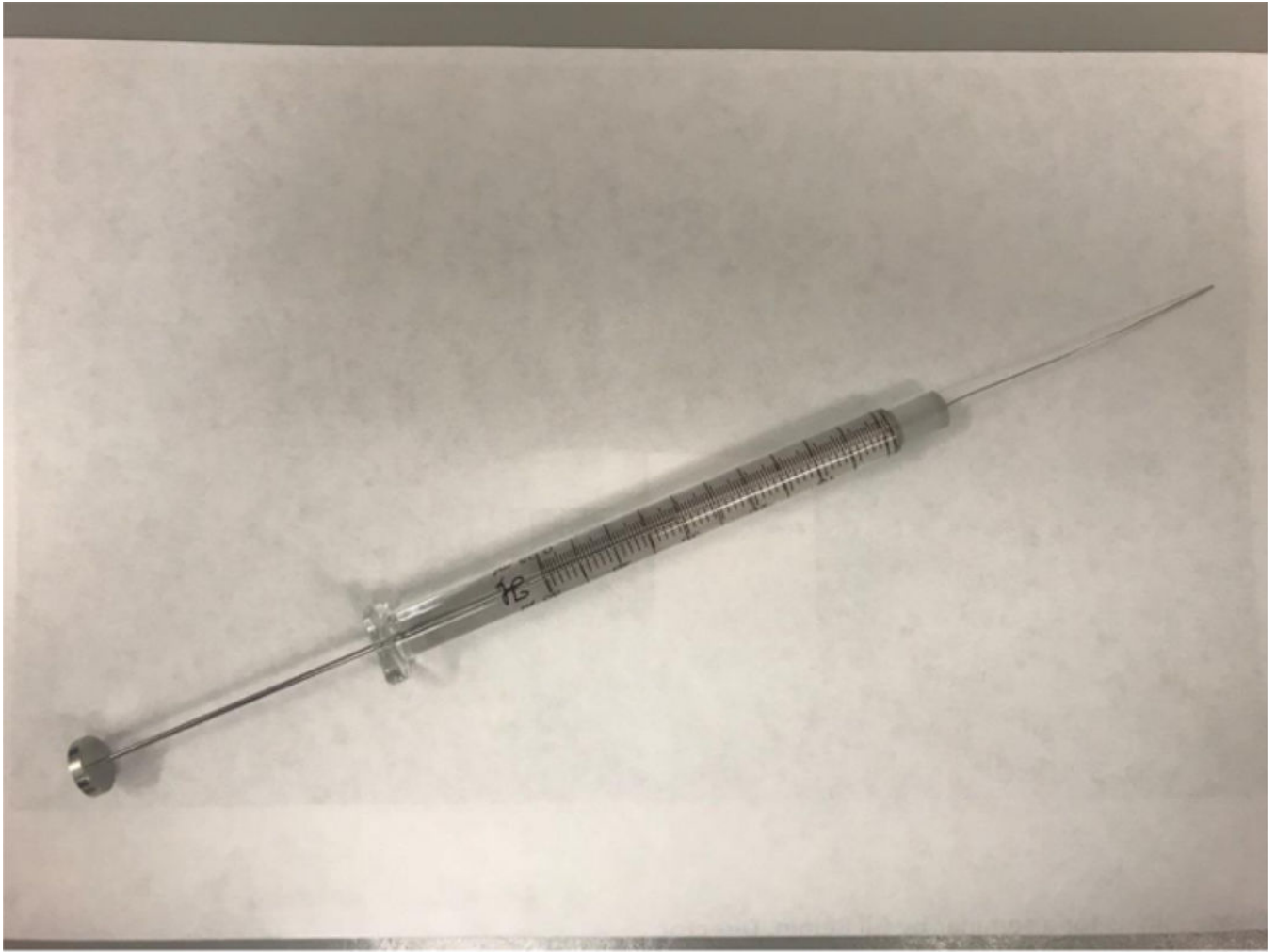


Figure 1. Syringe/needle setup used for intrahepatic injection.

The custom-made Hamilton 280508 syringe/needle setup includes a 30-gauge, 51-mm-long needle with a beveled edge and an attached 50- μ L glass syringe. Maximum injection volume in this procedure is 25 μ L.

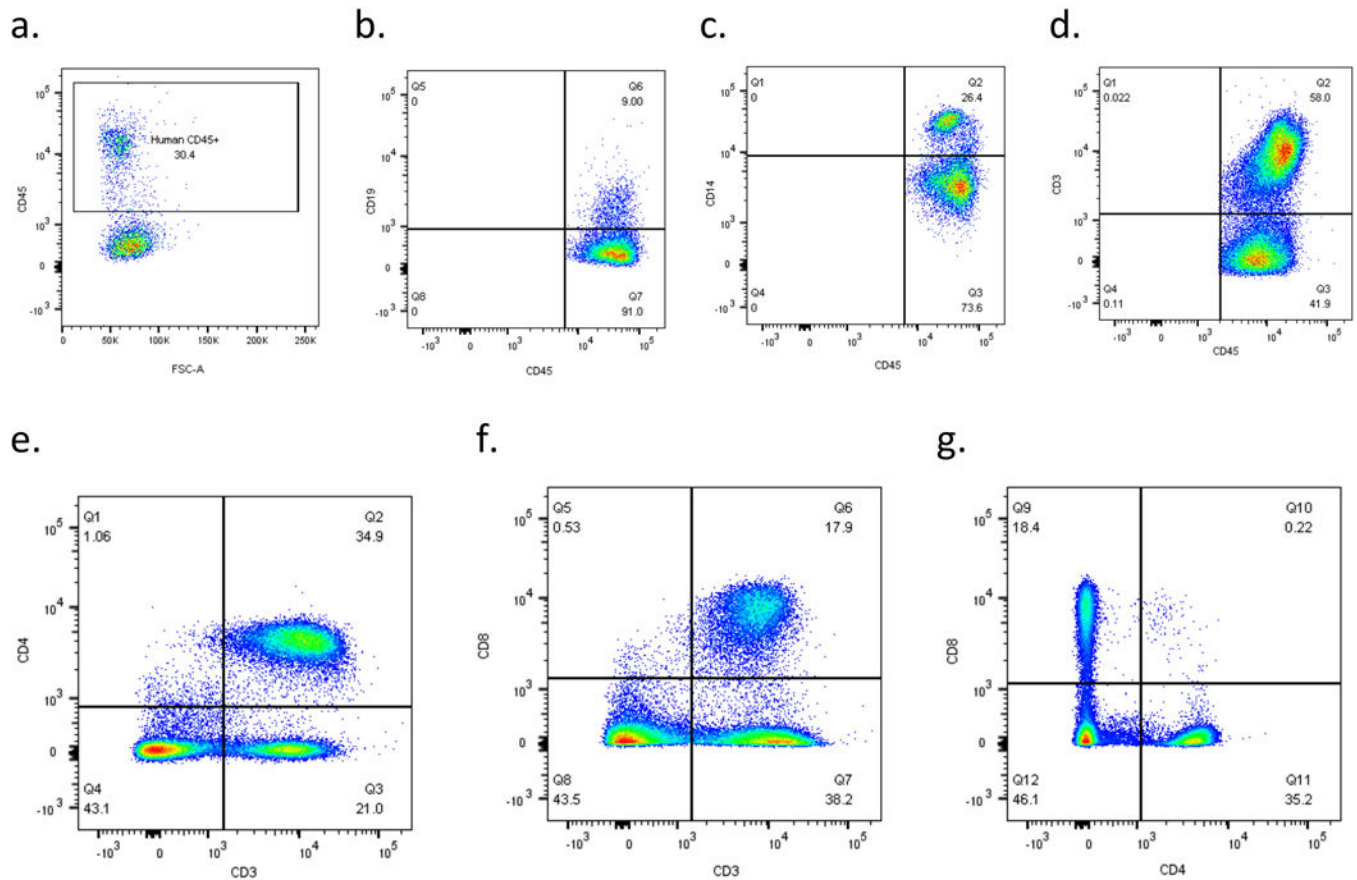


Figure 2. Flow cytometry data represent successful engraftment and the developments of lymphoid and myeloid cells in the peripheral blood.

Successfully prepared peripheral blood samples should have discrete population separations, and a well-engrafted hu-NSG mouse should have T-cell, B-cell and monocyte positive populations presented in the peripheral blood. A CD34:CD8 chart is recommended for ratio calculation. **a)** Successful engraftment showed more than 25% CD45+ human leukocytes in the peripheral blood; discrete population of **b)** B-cells, **c)** monocytes, **d)** T-cells among human CD45+ leukocyte; **e)** CD4+ helper T-cells and **f)** CD8+ cytotoxic T-cells are well separated, and **g)** yields a ratio between 1.5 to 2.5 in this uninfected hu-NSG.

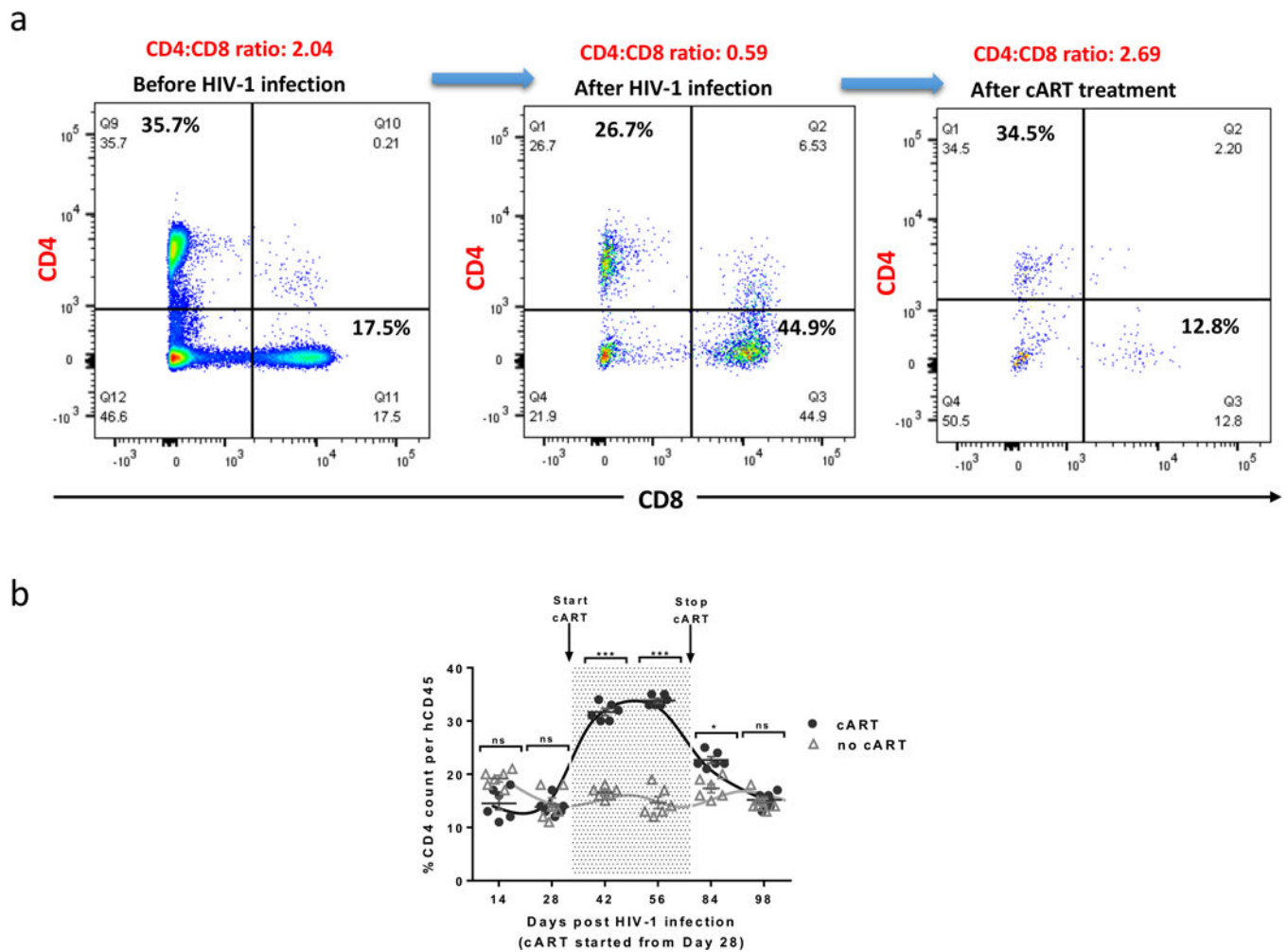


Figure 3. CD4⁺ cell count changes throughout the course of viral infection, cART and cART withdraw.

As infection progresses, the CD44:CD8 ratio decreases from 1.5–2.5 to >1.0, CD4:CD8 ratio has been served as a clinical parameter in evaluating HIV prognosis as well as treatment efficacies. **a)** Representative flow data indicating the change in CD4:CD8 ratios during the experimental course; **b)** Comparison trend chart indicating the effectiveness of cART, which can be identified as restored percentage of CD4⁺ T cells. Detection of CD4⁺ T cell count by flow cytometry. N: number of tested mice = 6; Error bars: means \pm SEM. * $p < 0.05$, ** $p < 0.01$, *** $p < 0.001$, **** $p < 0.0001$, ns: no significant different. Two-way ANOVA analysis is employed. Figure is reprinted with permission²².

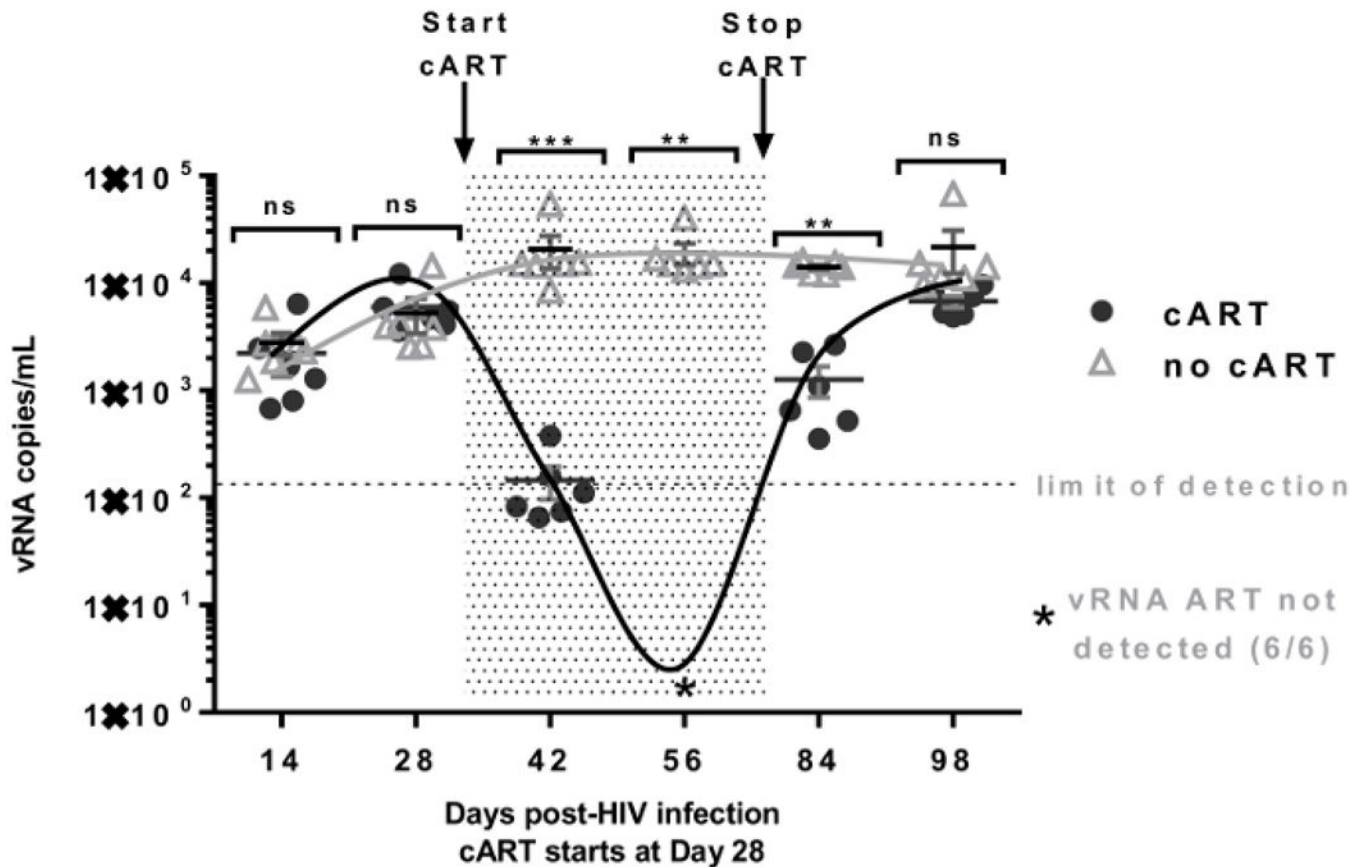


Figure 4. Changes of serum viral RNA copy numbers throughout the course of viral infection, cART and cART withdraw

Detection of plasma viremia in the HIV-infected hu-NSG mice by qRT-PCR. The shaded area indicates the time period during which the mice received cART (from Day 28 to Day 70 as shown). The limit of detection (indicated by the dashed line) of the PCR assay is (~110–160 RNA copies/mL) in 50 to 80 μ L of plasma obtained through the tail vein. Star (*) indicates viral RNA not detected in cART treated animals at Day 56. Serum viral RNA copy number analyzed from peripheral blood samples serves as direct evidence concerning the degree of viral infection. It should be in the agreement with the CD4 flow analysis. N: number of tested mice = 6; Error bars: means \pm SEM. * $p < 0.05$, ** $p < 0.01$, *** $p < 0.001$, **** $p < 0.0001$, ns: no significant different. Two-way ANOVA analysis is employed. Figure is reprinted with permission²².

Table 1.

Daily dose of individual medication in cART regimen

Medication	Daily Dose (mg)
Tenofovir disoproxil fumarate	300
Emtricitabine	200
Raltegravir	800

Author Manuscript

Author Manuscript

Author Manuscript

Author Manuscript

Table 2.

Weight, BSA and Km factor chart for dose conversion

Species	Weight (kg)	BSA (m ²)	K _m factor
Human			
Adult	60	1.6	37
Child	20	0.8	25
Mouse	0.02	0.0007	3

Author Manuscript

Author Manuscript

Author Manuscript

Author Manuscript

Table 3.

Blocking cocktail for isolated blood cells

Reagent	Volume (μ l) [*]	Final Concentration
0.01% BSA in PBS	98	
10 mg/ml human IgG	1	100 μ g/ml
10 mg/ml mouse IgG	1	100 μ g/ml
	100	

* Recipe is for one cell sample blocked in 100 μ l blocking cocktail. Adjust the volume accordingly with sample numbers.

Table 4.

Suggested multi-color flow panel

Antibody	Fluorophore	Ex. Max	Em. Max
CD45	BB515	490 nm	515 nm
CD3	PE-Cy7	496 nm	785 nm
CD4	Pacific Blue	401 nm	452 nm
CD8	BUV395	348 nm	395 nm
CD14	APC-Alexa 750	650 nm	774 nm
CD19	PE	496 nm	578 nm

Author Manuscript

Author Manuscript

Author Manuscript

Author Manuscript

Table 5.

HIV-1 LTR Primers and probe

Forward Primer	5'-GCCTCAATAAAGCTTGCCTTG-3'
Reverse Primer	5'-GGCGCCACTGCTAGAGATTTT-3'
Probe*	5'-AAGTAGTGTGTGCCCGTCTGTTAGTGTGACT-3'

* 5'-FAM, 3'-Black Hole Quenche 1

Author Manuscript

Author Manuscript

Author Manuscript

Author Manuscript

Materials

Name	Company	Catalog Number	Comments
CD34 MicroBead Kit, human	MiltenyiBiotec	130-046-703	
CryoStor CS2	Stemcell Technologies	07932	
NOD.Cg-Prkdc ^{scid} J12rg ^{tm1Wii}	The Jackson Laboratory	005557	Order breeders instead of experimental mice
IsoFlo	Patterson Veterinary	07-806-3204	Order through animal facility, restricted item
Clidox disinfectant	Fisher Scientific	NC9189926	
Wescodyne	Fisher Scientific	19-818-419	
Hamilton 80508 syringe/needle	Hamilton	80508	Custom made
Blood collection tube (K2EDTA)	BD Bioscience	367843	
Blood collection tube (Heparin)	BD Bioscience	365965	
Capillary tube (Heparinized)	Fisher Scientific	22-362574	
Red Blood Cell Lysis Buffer	Sigma Aldrich	11814389001	
QIAamp Viral RNA mini kit	Qiagen	52906	
TaqMan Fast Virus 1-step Master Mix	ThermoFisher	4444434	
HIV-1 P24 ELISA (5 Plate kit)	PerkinElmer	NEK050B001KT	
IgG from human serum	Sigma Aldrich	I4506-100MG	
IgG from mouse serum	Sigma Aldrich	I5381-10MG	
BB515 Mouse Anti-Human CD45 (clone HI30)	BD Biosciences	564586	RRID: AB_2732068, LOT 6347696
PE-Cy7 Mouse Anti-Human CD3 (Clone SK7)	BD Biosciences	557851	RRID: AB_396896, LOT 6021877
Pacific Blue Mouse Anti-Human CD4 (Clone RPA-T4)	BD Biosciences	558116	RRID: AB_397037, LOT 6224744
BUV395 Mouse Anti-Human CD8 (Clone RPA-T8)	BD Biosciences	563795	RRID: AB_2722501, LOT 6210668
APC-Alexa Fluor 750 Mouse Anti-Human CD14 (TuK4)	ThermoFisher	MHCD1427	RRID: AB_10373536, LOT 1684947A
PE Mouse Anti-Human CD19 (SJ25-C1)	ThermoFisher	MHCD1904	RRID: AB_10373382, LOT 1725304B